Different temperature dependence of carrier transport properties between $Al_xGa_{1-x}N/In_yGa_{1-y}N/GaN$ and $Al_xGa_{1-x}N/GaN$ heterostructures*

Song Jie (宋 杰), Xu Fu-Jun(许福军)†, Huang Cheng-Cheng(黄呈橙), Lin Fang(林 芳), Wang Xin-Qiang(王新强), Yang Zhi-Jian(杨志坚), and Shen Bo(沈 波)‡

State Key Laboratory of Artificial Microstructure and Mesoscopic Physics, School of Physics, Peking University, Beijing 100871, *China*

(Received 22 November 2010; revised manuscript received 7 January 2011)

The temperature dependence of carrier transport properties of $Al_xGa_{1-x}N/In_yGa_{1-y}N/GaN$ and $Al_xGa_{1-x}N/GaN$ heterostructures has been investigated. It is shown that the Hall mobility in $Al_{0.25}Ga_{0.75}N/In_{0.03}Ga_{0.97}N/GaN$ heterostructures is higher than that in $Al_{0.25}Ga_{0.75}N/GaN$ heterostructures at temperatures above 500 K, even the mobility in the former is much lower than that in the latter at 300 K. More importantly, the electron sheet density in $Al_{0.25}Ga_{0.75}N/In_{0.03}Ga_{0.97}N/GaN$ heterostructures decreases slightly, whereas the electron sheet density in $Al_{0.25}Ga_{0.75}N/GaN$ heterostructures gradually increases with increasing temperature above 500 K. It is believed that an electron depletion layer is formed due to the negative polarization charges at the $In_yGa_{1-y}N/GaN$ heterointerface induced by the compressive strain in the $In_yGa_{1-y}N$ channel, which effectively suppresses the parallel conductivity originating from the thermal excitation in the underlying GaN layer at high temperatures.

Keywords: temperature dependence, Hall mobility, parallel conductivity

PACS: 73.61.Ey, 72.20.Fr, 73.50.Dn, 73.40.Kp **DOI:** 10.1088/1674-1056/20/5/057305

1. Introduction

GaN-based high electron mobility transistors (HEMTs) with $In_xGa_{1-x}N$ channels play an important role in suppressing low frequency noise and current collapse because of the excellent carrier confinement.[1,2] Due to the larger conduction band offset (CBO) and higher polarization charge density at the $Al_xGa_{1-x}N/In_yGa_{1-y}N$ heterointerface, there is generally higher two-dimensional electron gas (2DEG) density in $Al_xGa_{1-x}N/In_yGa_{1-y}N/GaN$ heterostructures compared to conventional $Al_xGa_{1-x}N/GaN$ ones.[3] Currently, there are many experiments studying $In_yGa_{1-y}N$-channel-based heterostructures, including the material growth and the device fabrication. For example, Okamoto *et al.* obtained the $Al_xGa_{1-x}N/In_yGa_{1-y}N/GaN$ heterostructures with the 2DEG mobility of 1110 $cm^2/(V\cdot s)$ and the sheet carrier density of 1.31×10^{13} cm^{-2} at room temperature (RT) by using a 3-nm thick $In_{0.06}Ga_{0.94}N$ channel layer.[4] Xie *et al.* reported that the electron mobility of $In_{0.04}Ga_{0.96}N$ channel HEMTs could be improved by using an $Al_{0.24}In_{0.01}Ga_{0.75}N$ barrier and obtained the heterostructures with the 2DEG mobility of 1230 $cm^2/(V\cdot s)$ and sheet electron density of 1.09×10^{13} cm^{-2} at RT.[5] Besides, Lanford *et al.* reported that AlGaN/InGaN/GaN HEMTs could improve the electron transport characteristics by suppressing the current collapse and obtained the high performance devices with a cutoff frequency of 17.3 GHz and a maximum frequency of 28.7 GHz.[6] Though many progresses have been achieved, there are still many questions needing further investigation, especially the carrier transport properties of $In_yGa_{1-y}N$ channel HEMTs at high temperatures. Due to its importance in high temperature and high frequency application, the study of temperature dependence of electrical transport properties in $In_yGa_{1-y}N$ channel HEMTs is very necessary and essential.

In this study, temperature dependence of the carrier transport properties in $Al_xGa_{1-x}N/In_yGa_{1-y}N/$

*Project supported by the National Natural Science Foundation of China (Grant Nos. 60906041, 60736033, 60890193, and 10774001).

†Corresponding author. E-mail: fjxu@pku.edu.cn

‡Corresponding author. E-mail: bshen@pku.edu.cn

© 2011 Chinese Physical Society and IOP Publishing Ltd

GaN and $Al_xGa_{1-x}N$/GaN heterostructures has been investigated. The stronger carrier confinement effect has been observed in $Al_xGa_{1-x}N/In_yGa_{1-y}N$/GaN heterostructures compared to that in conventional $Al_xGa_{1-x}N$/GaN heterostructures at high temperatures.

2. Experiment

$Al_xGa_{1-x}N/In_yGa_{1-y}N$/GaN and $Al_xGa_{1-x}N$/GaN heterostructures used in this study were grown on 50.8 mm (0001) sapphire substrates by metal-organic chemical vapour deposition (MOCVD) with a Thomas Swan close coupled showerhead system. Trimethylgallium, trimethylaluminum, trimethylindium and ammonia were used as Ga, Al, In and N sources, respectively. The growth process initiated by a 530 °C GaN nucleation layer, followed by a 2-μm thick unintentionally doped GaN buffer layer at 1060 °C under H_2 atmosphere. Then the wafer was cooled down to 780 °C for growing the 10-nm thick $In_yGa_{1-y}N$ channel under N_2 ambient. The thickness of the $In_yGa_{1-y}N$ layer was controlled by growth time. Then a 1.5-nm thick AlN layer was grown at 780 °C to protect the $In_yGa_{1-y}N$ channel. After that, the wafer was heated to 1080 °C and about 25-nm thick $Al_xGa_{1-x}N$ ($x = 0.25$) barrier layer was grown. Correspondingly, the $Al_xGa_{1-x}N$/GaN ($x = 0.25$) heterostructure samples were grown under the same conditions, including the GaN buffer layer and $Al_xGa_{1-x}N$ ($x = 0.25$) barrier. A 1.5-nm thick AlN interlayer was also grown on GaN at 1080 °C before the barrier growth. Besides, a 2-μm thick as-grown GaN epilayer was also prepared under the same growth condition as the GaN buffer layers in the heterostructures.

After the growth, the carrier mobility and sheet density were obtained by Hall effect measurements using van der Pauw geometry. Square-shaped samples (5×5 mm^2) were prepared with four evapourated circular Ti/Al/Ni/Au ohmic contact electrodes at the four corners. The Ti/Al/Ni/Au electrodes were annealed at 850 °C for 35 s to ensure good ohmic contacts. The thickness and In content of the $In_yGa_{1-y}N$ channel were evaluated by high-resolution X-ray diffraction (XRD).

3. Results and discussion

Figure 1 shows the typical XRD ω–2θ scan of an $Al_{0.25}Ga_{0.75}N/In_{0.03}Ga_{0.97}N$/GaN heterostructure sample. The In content of $In_yGa_{1-y}N$ channel is determined to be about 0.03 by simulations. As shown in Fig. 1, thickness fringes are clearly seen in the curve, which indicates that the samples are of high crystalline quality.

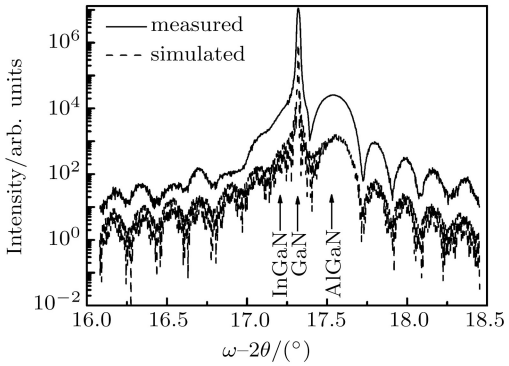


Fig. 1. The measured and simulated high-resolution X-ray diffraction (002) ω–2θ scans of a typical $Al_{0.25}Ga_{0.75}N/In_{0.03}Ga_{0.97}N$/GaN heterostructure.

Figure 2 shows the temperature dependence of the electron mobility from 100 to 500 K in the typical $Al_{0.25}Ga_{0.75}N/In_{0.03}Ga_{0.97}N$/GaN and $Al_{0.25}Ga_{0.75}N$/GaN samples. The mobility in the $Al_{0.25}Ga_{0.75}N/In_{0.03}Ga_{0.97}N$/GaN sample is 918 cm^2/(V·s) at 300 K and increases to 1920 cm^2/(V·s) with decreasing temperature to 100 K. In contrast, the mobility in the $Al_{0.25}Ga_{0.75}N$/GaN sample is 1420 cm^2/(V·s) at 300 K, and rapidly increases to 7730 cm^2/(V·s) at 100 K. These results indicate that the increased scattering to the electrons in $Al_xGa_{1-x}N/In_yGa_{1-y}N$/GaN heterostructures is stronger than that in $Al_xGa_{1-x}N$/GaN ones, which should be ascribed to the worse heterointerface and the increasing contribution of alloy scattering in the $In_yGa_{1-y}N$ channel itself.[5]

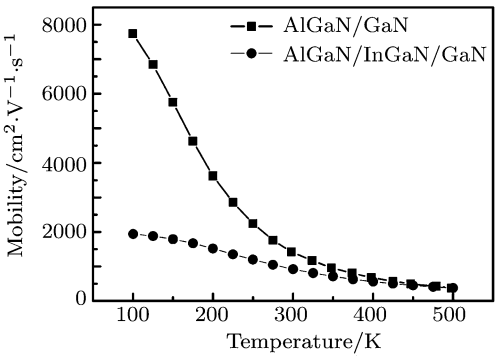


Fig. 2. The temperature dependence of the electron mobility in the $Al_{0.25}Ga_{0.75}N/In_{0.03}Ga_{0.97}N$/GaN and $Al_{0.25}Ga_{0.75}N$/GaN heterostructures from 100 to 500 K.

Then we further compare the temperature dependence of the electrical properties in these two

heterostructure samples at temperatures higher than 300 K. For comparison, electrical properties of the GaN epilayer were also measured. As shown in Fig. 3(a), the measured Hall mobility in the $Al_{0.25}Ga_{0.75}N/In_{0.03}Ga_{0.97}N/GaN$ sample gradually decreases with increasing temperature, as for the case of the $Al_{0.25}Ga_{0.75}N/GaN$ sample. However, it is noticeable that the Hall mobility in the $Al_{0.25}Ga_{0.75}N/In_{0.03}Ga_{0.97}N/GaN$ sample is higher than that in the $Al_{0.25}Ga_{0.75}N/GaN$ one when the temperature is higher than 500 K. More importantly, it can be seen in Fig. 3(b) that the measured electron sheet density of $Al_{0.25}Ga_{0.75}N/GaN$ sample decreases with increasing temperature from 300 to 500 K and then gradually increases with increasing temperature above 500 K, presenting a nonmonotonic variation trend. In contrast, the electron sheet density in the $Al_{0.25}Ga_{0.75}N/In_{0.03}Ga_{0.97}N/GaN$ sample decreases slightly with increasing temperature above 500 K, exhibiting a very weak temperature dependence, which is completely different from that of the $Al_{0.25}Ga_{0.75}N/GaN$ sample.

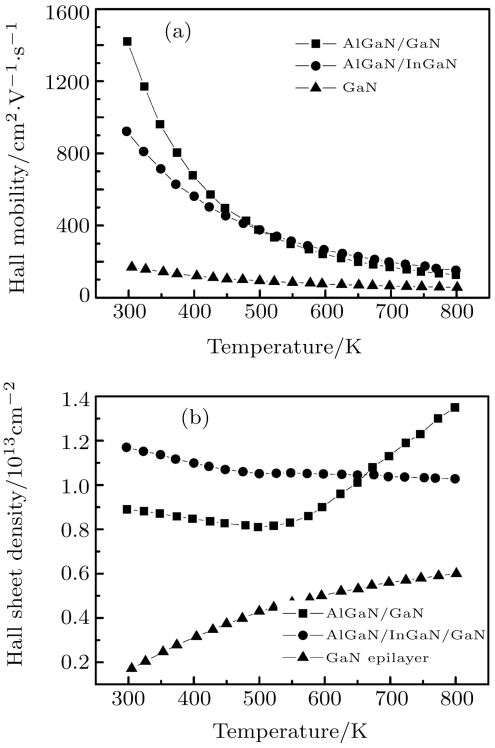


Fig. 3. Temperature dependence of the electron mobility and sheet density in $Al_{0.25}Ga_{0.75}N/In_{0.03}Ga_{0.97}N/GaN$, $Al_{0.25}Ga_{0.75}N/GaN$ heterostructures and GaN epilayer from 300 K to 800 K: (a) Hall mobility and (b) sheet density.

In order to better understand the intrinsic mechanisms contributing to the different temperature dependence of the electrical properties in these two kinds of heterostructures, the schematic conduction band diagram of $Al_xGa_{1-x}N/In_yGa_{1-y}N/GaN$ and $Al_xGa_{1-x}N/GaN$ heterostructures are shown in Fig. 4. In $Al_xGa_{1-x}N/GaN$ heterostructures, the spontaneous polarisation (P_{sp}) and piezoelectric polarization (P_{pe}) in the $Al_xGa_{1-x}N$ barrier are aligned parallel and pointing to the substrate due to the tensile strain in the $Al_xGa_{1-x}N$ barrier, which is the same as the P_{sp} in GaN, as shown in Fig. 4(c). This should cause net positive polarisation charges σ^+ cumulated at the $Al_xGa_{1-x}N/GaN$ heterointerface

$$\begin{aligned}\sigma^+(\mathrm{AlGaN/GaN}) &= |P(\mathrm{top}) - P(\mathrm{bottom})| \\ &= |\{P_{sp}(\mathrm{AlGaN}) + P_{pe}(\mathrm{AlGaN})\} \\ &\quad - \{P_{sp}(\mathrm{GaN})\}|. \end{aligned} \tag{1}$$

Adopting the material parameters and formulas listed in Ref. [7], the parameters of $Al_{0.25}Ga_{0.75}N$ and $In_{0.03}Ga_{0.97}N$ are obtained adopting a linear interpolation technique. The polarisation charges density at $Al_{0.25}Ga_{0.75}N/GaN$ interface is estimated to be $\sigma^+(\mathrm{AlGaN/GaN}) = 0.02222$ C/m^2.

In $Al_xGa_{1-x}N/In_yGa_{1-y}N/GaN$ heterostructures, the P_{pe} in $In_yGa_{1-y}N$ channel is antiparallel to the P_{pe} in $Al_xGa_{1-x}N$ barrier due to the compressive strain in $In_yGa_{1-y}N$ channel, as shown in Fig. 4(d), which should cause the net positive polarization charges σ^+ cumulated at the $Al_xGa_{1-x}N/In_yGa_{1-y}N$ heterointerface

$$\begin{aligned}&\sigma^+(\mathrm{AlGaN/InGaN}) \\ &= |P_{sp}(\mathrm{AlGaN}) + P_{pe}(\mathrm{AlGaN}) - P_{pe}(\mathrm{InGaN}) \\ &\quad - P_{sp}(\mathrm{InGaN})|. \end{aligned} \tag{2}$$

The polarization charges density at the $Al_{0.25}Ga_{0.75}N/In_{0.03}Ga_{0.97}N$ heterointerface is estimated to be $\sigma^+(\mathrm{AlGaN/InGaN}) = 0.02661$ C/m^2. Meanwhile, there should be net negative polarisation charges σ^- cumulated at the $In_yGa_{1-y}N/GaN$ heterointerface

$$\begin{aligned}\sigma^-(\mathrm{InGaN/GaN}) = &- |P_{sp}(\mathrm{GaN}) - \mathrm{P}_{pe}(\mathrm{InGaN}) \\ &- P_{sp}(\mathrm{InGaN})|. \end{aligned} \tag{3}$$

The polarization charges density at $In_{0.03}Ga_{0.97}N/GaN$ interface is estimated to be $\sigma^-(\mathrm{InGaN/GaN}) = -0.00439$ C/m^2. Thus, there should be a carrier depletion layer formed near the $In_yGa_{1-y}N/GaN$ heterointerface in heterostructures of $Al_xGa_{1-x}N/In_yGa_{1-y}N/GaN$, which is significantly different from that in those of $Al_xGa_{1-x}N/GaN$, as shown in Figs. 4(a) and 4(b). This depletion layer can prevent the electrons transport from underlying GaN to 2DEG channel and enhance the electron confinement in the channel.

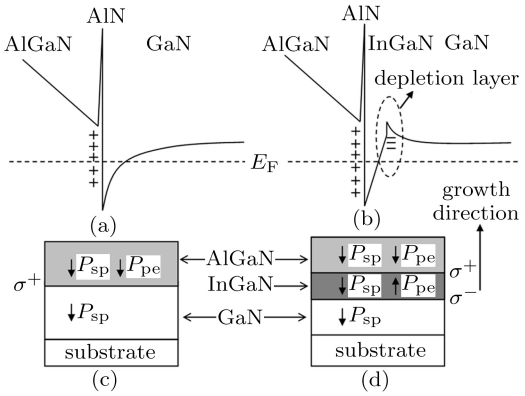


Fig. 4. Schematic conduction band diagrams and directions of spontaneous and piezoelectric polarizations in $Al_xGa_{1-x}N$/GaN and $Al_xGa_{1-x}N/In_yGa_{1-y}N$/GaN heterostructures. (a) $Al_xGa_{1-x}N$/GaN conduction band, (b) $Al_xGa_{1-x}N/In_yGa_{1-y}N$/GaN conduction band, (c) directions in $Al_xGa_{1-x}N$/GaN, (d) directions in $Al_xGa_{1-x}N/In_yGa_{1-y}N$/GaN.

The principle of Hall measurement is further analysed to understand the different temperature dependence of the electrical properties between $Al_xGa_{1-x}N$/GaN and $Al_xGa_{1-x}N/In_yGa_{1-y}N$/GaN heterostructures. In general, the measured Hall conductivity in $Al_xGa_{1-x}N$/GaN and $Al_xGa_{1-x}N/In_yGa_{1-y}N$/GaN heterostructures is contributed to both from the 2DEG channel and electrons in the underlying GaN layer. The measured Hall sheet carrier density and mobility can be expressed as[8]

$$n_H\mu_H = n_{2DEG}\mu_{2DEG} + n_{GaN}\mu_{GaN}, \tag{4}$$

where n_H and μ_H represent the measured Hall sheet carrier density and mobility, n_{2DEG} and μ_{2DEG} represent the actual sheet 2DEG density and mobility and n_{GaN} and μ_{GaN} represent the sheet electron concentration and mobility of the underlying GaN layer, respectively. The n_H and μ_H are given by the following expressions:[8]

$$n_H = \frac{(n_{2DEG}\mu_{2DEG} + n_{GaN}\mu_{GaN})^2}{n_{2DEG}\mu_{2DEG}^2 + n_{GaN}\mu_{GaN}^2}, \tag{5}$$

and

$$\mu_H = \frac{n_{2DEG}\mu_{2DEG}^2 + n_{GaN}\mu_{GaN}^2}{n_{2DEG}\mu_{2DEG} + n_{GaN}\mu_{GaN}}. \tag{6}$$

As shown in Fig. 3, the Hall mobility in GaN epilayer is much lower than those in the $Al_xGa_{1-x}N$/GaN and $Al_xGa_{1-x}N/In_yGa_{1-y}N$/GaN samples, suggesting that the electron mobility in GaN epilayer is much lower than that of the channel 2DEG in heterostructures ($\mu_{GaN} < \mu_{2DEG}$). Thus, it can be deduced that μ_H is greater than μ_{GaN} and is less than μ_{2DEG} ($\mu_{GaN} < \mu_H < \mu_{2DEG}$) in $Al_xGa_{1-x}N$/GaN heterostructures because of the contribution from underlying GaN layer. Different from the case in $Al_xGa_{1-x}N$/GaN heterostructures, the measured Hall mobility and sheet density reflect the actual 2DEG in $Al_xGa_{1-x}N/In_yGa_{1-y}N$/GaN heterostructures owing to the depletion layer acting as high resistive zone as discussed above. Thus, the Hall mobility μ_H in $Al_xGa_{1-x}N/In_yGa_{1-y}N$/GaN heterostructures is close to the actual 2DEG mobility μ_{2DEG}. At temperatures above 500 K, because of the increasing contribution from underlying GaN layer, the measured Hall mobility in $Al_xGa_{1-x}N$/GaN heterostructures becomes lower than that in $Al_xGa_{1-x}N/In_yGa_{1-y}N$/GaN ones. Furthermore, in $Al_xGa_{1-x}N$/GaN heterostructures, the increased contribution of electron concentration originating from thermal excitation in the underlying GaN layer accounts for the increase of sheet density with increasing temperature above 500 K.[9–11] But in $Al_xGa_{1-x}N/In_yGa_{1-y}N$/GaN heterostructures, the contribution of the parallel conductivity in the underlying GaN layer is suppressed by the depletion layer. The measured sheet density is mainly determined by actual 2DEG concentration ($n_H \approx n_{2DEG}$) and thus slightly decreases with increasing temperature above 500 K.

In addition, we have further analysed the factors influencing the 2DEG density in these two types of heterostructures, such as conduction band offsets (CBOs) and P_{pe} in $Al_xGa_{1-x}N$ barrier and $In_yGa_{1-y}N$ channel layer. Adopting the same method, we have reported previously[9] that the variations of the CBOs in $Al_{0.25}Ga_{0.75}N/In_{0.03}Ga_{0.97}N$ and $Al_{0.25}Ga_{0.75}N$/GaN from 300 to 800 K have been calculated using the parameters in Ref. [12]–[14]. When the temperature increases from 300 to 800 K, the CBOs for $Al_{0.25}Ga_{0.75}N/In_{0.03}Ga_{0.97}N$ and $Al_{0.25}Ga_{0.75}N$/GaN heterostructures reduce by 0.032 and 0.029 eV, respectively. The difference is only 0.003 eV. This indicates that the reduction of the 2DEG density due to the decrease of CBO is not the key leading to the different temperature dependence between $Al_{0.25}Ga_{0.75}N/In_{0.03}Ga_{0.97}N$ and $Al_{0.25}Ga_{0.75}N$/GaN heterostructures. Meanwhile, we have also analysed the change of the 2DEG concentration resulting from temperature dependent strain

in the $Al_{0.25}Ga_{0.75}N$ barrier from 300 to 800 K by considering the spontaneous and piezoelectric polarisation charges and find that the change of the 2DEG concentration is very little. In fact, Chen *et al.* once reported that 2DEG concentration decreased about 4% from 300 to 800 K induced by the change of P_{pe} in $Al_{0.22}Ga_{0.78}N$ barrier.[15] Therefore, the effect originating from variations of P_{pe} at different temperatures in these two types of heterostructures can be neglected.

Based on the above analysis, it is believed that the primary factor leading to the different temperature dependence of the carrier transport properties in $Al_xGa_{1-x}N/In_yGa_{1-y}N/GaN$ and $Al_xGa_{1-x}N/GaN$ heterostructures is the depletion layer formed at the $In_yGa_{1-y}N/GaN$ heterointerface. This depletion layer can effectively suppress the parallel conductivity effect in the underlying GaN layer and provide better carrier confinement, which can improve the buffer isolation and enhance the stability of HEMT devices, especially at high temperatures.

4. Conclusion

In conclusion, we have investigated the temperature dependence of carrier transport properties of $Al_xGa_{1-x}N/In_yGa_{1-y}N/GaN$ and $Al_xGa_{1-x}N/GaN$ heterostructures. It is shown that the Hall mobility in $Al_{0.25}Ga_{0.75}N/In_{0.03}Ga_{0.97}N/$ GaN heterostructures is higher than that in $Al_{0.25}Ga_{0.75}N/GaN$ at temperatures above 500 K. More importantly, the electron sheet density in $Al_{0.25}Ga_{0.75}N/In_{0.03}Ga_{0.97}N/GaN$ heterostructures decreases slightly with increasing temperature above 500 K, whereas the electron sheet density in $Al_{0.25}Ga_{0.75}N/GaN$ heterostructures gradually increases with increasing temperature above 500 K. We believe that an electron depletion layer is formed owing to the negative piezoelectric polarisation charges at the $In_yGa_{1-y}N/GaN$ heterointerface induced by the compressive strain in the $In_yGa_{1-y}N$ channel, which effectively suppresses the parallel conductivity originating from the thermal excitation in the underlying GaN layer at high temperatures.

References

[1] Simin G, Hu X, Tarakji A, Zhang J, Koudymov A, Saygi S, Yang J, Khan M A, Shur M S and Gaska R 2001 *Jpn. J. Appl. Phys.* **40** L1142

[2] Pala N, Rumyantsev S, Shur M, Gaska R, Hu X, Yang J, Simin G and Khan M A 2003 *Solid State Electron.* **47** 1099

[3] Wang C X, Tsubaki K, Kobayashi N, Makimato T and Maeda N 2004 *Appl. Phys. Lett.* **84** 2313

[4] Okamoto N, Hoshino K, Hara N, Takikawa M and Arakawa Y 2004 *J. Cryst. Growth* **272** 278

[5] Xie J, Leach J H, Ni X, Wu M, Shimada R, Özgür Ü and Morkoç H 2007 *Appl. Phys. Lett.* **91** 262102

[6] Lanford W, Kumar V, Schwindt R, Kuliev A, Adesida I, Dabiran A M, Wowchak A M, Chow P P and Lee J W 2004 *IEEE Electron. Lett.* **40** 771

[7] Ambacher O, Smart J, Shealy J R, Weimann N G, Chu K, Murphy M, Dimitrov R, Wittmer L and Stutzmann M, Rieger W and Hilsenbeck J 1999 *J. Appl. Phys.* **85** 3222

[8] Look D C and Molnar R J 1997 *Appl. Phys. Lett.* **70** 3377

[9] Wang M J, Shen B, Xu F J, Wang Y, Xu J, Huang S, Yang Z J, Qin Z X and Zhang G Y 2007 *Appl. Phys.* A **88** 715

[10] Dziuba Z, Antoszewski J, Dell J M, Faraone L, Kozodoy P, Keller S, Keller B, DenBaars S P and Mishra U K 1997 *J. Appl. Phys.* **82** 2996

[11] Siekacz M, Dybko K, Skierbiszewski C, Knap W, Wasilewski Z, Maude D, Sakowski J, Krupczyński W, Nowak G, Boćkowski M and Porowski S 2005 *Phys. Stat. Sol.* (c) **2** 1355

[12] Nepal N, Li J, Nakarmi M L, Lin J Y and Jiang H X 2001 *Appl. Phys. Lett.* **79** 2270

[13] Wu J, Walukiewicz W, Shan W, Yu K M, Ager J W, Li S X, Haller E E, Lu H and Schaff W J 2003 *J. Appl. Phys.* **94** 4457

[14] Wu J 2009 *J. Appl. Phys.* **106** 011101

[15] Chen D J, Zhang K X, Tao Y Q, Wu X S, Xu J, Zhang R, Zheng Y D and Shen B 2006 *Appl. Phys. Lett.* **88** 102106